11-2018

Erosion Rate Equations for Coarse- Grained Materials Using a Small Flume Testing

Ghada Ellithy
Embry-Riddle Aeronautical University, Ghada.Ellithy@erau.edu

Johannes L. Wibowo
USACE

Maureen K. Corcoran
Vicksburg MS

Erosion Rate Equations for Coarse- Grained Materials Using a Small Flume Testing

Ghada S. Ellithy[1], Johannes L. Wibowo[2], Maureen K. Corcoran[3].

Affiliation: [1,2, 3]Engineer Research and Development Center, USACE, Vicksburg MS.

ABSTRACT

Erosion rate of soils during a levee or dam overtopping event is a major component in risk assessment evaluation of breach time and consequently in determining the downstream consequences. There is uncertainty in estimation of the erosion rate especially for coarse-grained materials that comprise the outer shell layer of dams as well as homogenous levees that are constructed of such materials. In this paper, erosion rate results are presented on three soil mixes that share the same median grain size D_{50} of 2 mm, the fines content varies between zero and 20%, and the gravel content between zero and 30%. Each of the three mixes is compacted in the box at optimum or near optimum moisture content as determined from standard Proctor test. The box measures 0.3 m wide x 0.6 m long x 0.15 m deep. Each material is tested several times at varying hydraulic loading to determine the erosion rate after equal time intervals. The water depth, velocity are measured at each hydraulic loading and the acting bed shear is calculated. The validity of the excess shear stress equation is discussed as well as other bilinear and nonlinear models that could fit the erosion rate of such materials as it relates to the acting bed shear stress. The effect of fines content and level of acting shear stresses are presented in the paper.

INTRODUCTION

This paper presents the results from soil erosion testing performed in a small flume on three compacted soil mixes. The soil mixes are sand with varying contents of fines and clay contents compacted in a box that was placed within a 0.33 m wide flume. Four box samples were tested for each soil mix, each at a different flow level where the water depth and velocity measurements were taken at different stations along the flume and on top of the box. Water depth, velocity and bed shear were calculated using a discrete form of energy equation (Hughes, 2017).

For flood risk assessment of both dams and levees, the earthen structures are assumed to breach when they are overtopped. However, for a more accurate assessment and to estimate a realistic time and width of breach, more understanding of the erosion rate and mechanism is needed especially for coarse-grained (typically non-cohesive) sand and gravel materials. For coarse-grained materials, the response of the particles to the hydraulic loading is mainly affected by the size, shape, and density of particles, while for the finer cohesive materials the response is affected by the cohesive bonding of the particles. The response of a mix of the two types of soils is governed by the relative fractions of the cohesive and non-cohesive particles.

The generally accepted mathematical representation that describes the physical phenomena of erosion states that the rate of erosion is proportional to the difference in effective hydraulic shear stress and critical stress as adjusted by some coefficient of erosion. The erosion rate is generally expressed as (Hanson 1990):

$$\varepsilon_r = k_d \ (\tau - \tau_{cr})^a \quad (1)$$

where:

ε_r erosion rate (cm sec^{-1})

k_d erodibility coefficient (cm/sec)/(N/cm^2) or (cm^3/N-sec)

τ average hydraulic boundary shear stress (Pa)

τ_{cr} critical shear stress (Pa), and

a an empirical exponent

The erosion parameters, k_d and τ_{cr}, of coarse-grained material used in breach models are lacking in the literature because of the size of testing equipment and flow velocity required to capture these parameters. The values of both parameters depend on the index and engineering properties of the soil materials. The exponent a is commonly assumed to be unity (Hanson 1990; Hanson and Cook 1997) assuming a linear relationship. If the relationship between erosion rate and acting boundary shear is not linear, in other words when a is not unity, Equation 1 becomes unbalanced in units. In this paper, the erosion rate versus bed shear results are plotted against the acting bed shear stress, linear, bilinear and nonlinear equations is fitted on the results.

MATERIAL PROPERTIES

Grain Size. The study was performed on three sand mixes that maintain a D_{50} of about 2 mm. Sands of different grains size distributions, pea gravel, silt, and kaolin clay materials were mixed in different portions to produce the three mixes. Figure shows the grain size distribution of the three mixes 1-1, 1-2, and 1-3. For mixes 1-2, and 1-3, the addition of the silt and clay increased the fines content to about 5 and 20 percent and about 2 to 10 percent clay fraction (<2 μm), respectively. The gravel content in the three mixes varied between 23% and 30%. The uniformity coefficient: $C_u = D_{60}/D_{10}$, for the three mixes were greater than 6, however, only mix 1-1 has a curvature coefficient; $C_c = DD_{30}/D_{10} \times D_{60}$, that is between 1 and 3, indicating that only mix 1-1 is considered well graded material. In mixes 1-2 and 1-3, the plasticity index (PI) for the fraction passing sieve #40 was measured at 8% with a liquid limit LL of 30%, and a plastic limit PL of 22%. Based on the above, mixes 1-1, 1-2, and 1-3 could be classified according to the unified soil classification system (USCS) as well graded sand (SW), well graded sand-silty sand (SW-SM), and clayey sand (SC), respectively.

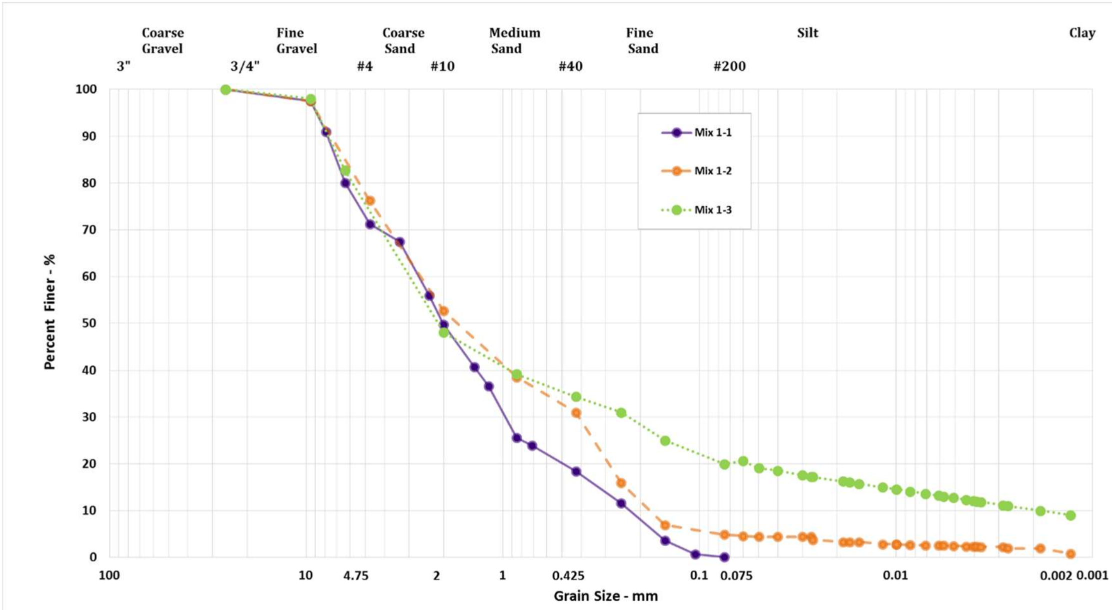

Figure 1. Grain size distribution for soil mixes 1-1, 1-2, and 1-3

Density. To prepare the three mixes, compaction was performed according to the standard Proctor test (ASTM D698-12) as shown in Figure . The dry density of the mixes increased with the fines content, however, the optimum water content remained within a narrow range between 6 and 7 percent. For evaluation of erosion, density conditions were selected near optimum as follows: water content; w_c = 6%, 7%, 7%, and dry density; γ_d = 127 pcf, 135 pcf, and 137 pcf for mixes 1-1, 1-2, and 1-3, respectively.

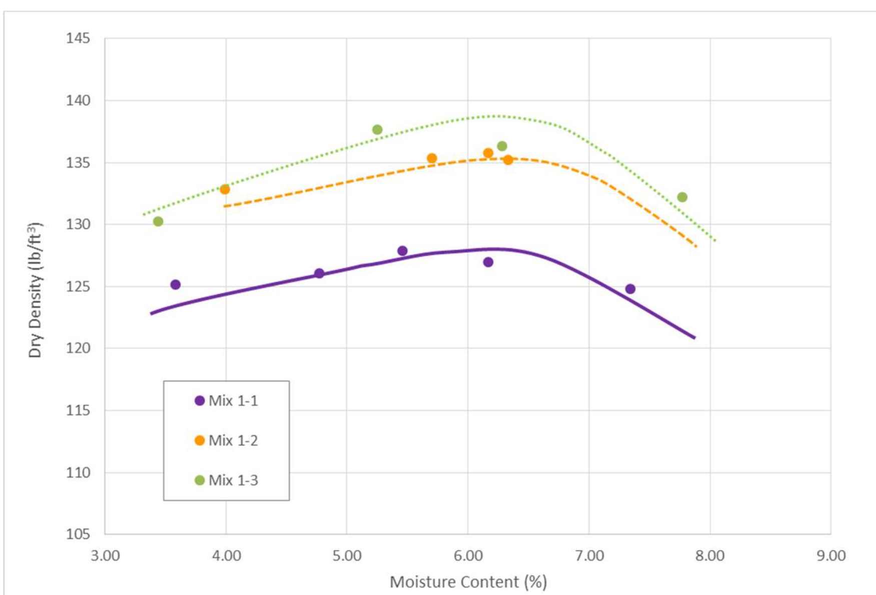

Figure 2. Compaction curves for soil mixes 1,2 ,3 and 4 using Standard Proctor (ASTM D-698).

SMALL FLUME TESTING

The small flume that was used in this study measured about 3.65 m (12 feet) in length, 0.33 m (1 foot) in width and 0.45 m (1.5 feet) in height, Figure 3. The flow was enabled through a pump that circulates water from an underneath storage tank. The pump could be adjusted to give varying flow levels, and the flume bed could be tilted up to 10% (about 5 degrees) to achieve higher velocities at the same flow level. A flow ranging from 0.0028 to 0.028 m^3/sec (0.1-1 cfs) was used in performing the erosion tests discussed in this paper. The box measures 0.33 m (1 foot) wide x 0.67 m (2 feet) long x 0.15 m (0.5 foot) high. The soil sample was compacted in the box in three lifts, with calculated volume and weight to match the corresponding density and water content for each mix as discussed above. The box was then inserted into a fitted space within the flume where it was epoxied overnight.

Before the test was started, the pump was adjusted to a selected flow level, and the flume bed to a tilting angle. The flow continued in each test for a duration of about 20 to 40 minutes after which sample erosion reached an almost equilibrium condition where the erosion progress stopped or very slow erosion occurred. The velocity was measured using a Pitot tube using the difference between the total and static head, and the water depth equaled static head. These measurements were taken at different locations along the flume as well as on top of the box sample. Manual readings using caliber and velocimeter were taken as well. Soil erosion profile for each test was created by measuring the erosion depth after the test was stopped using a measuring rod every inch along the centerline of the box, Figure 4.

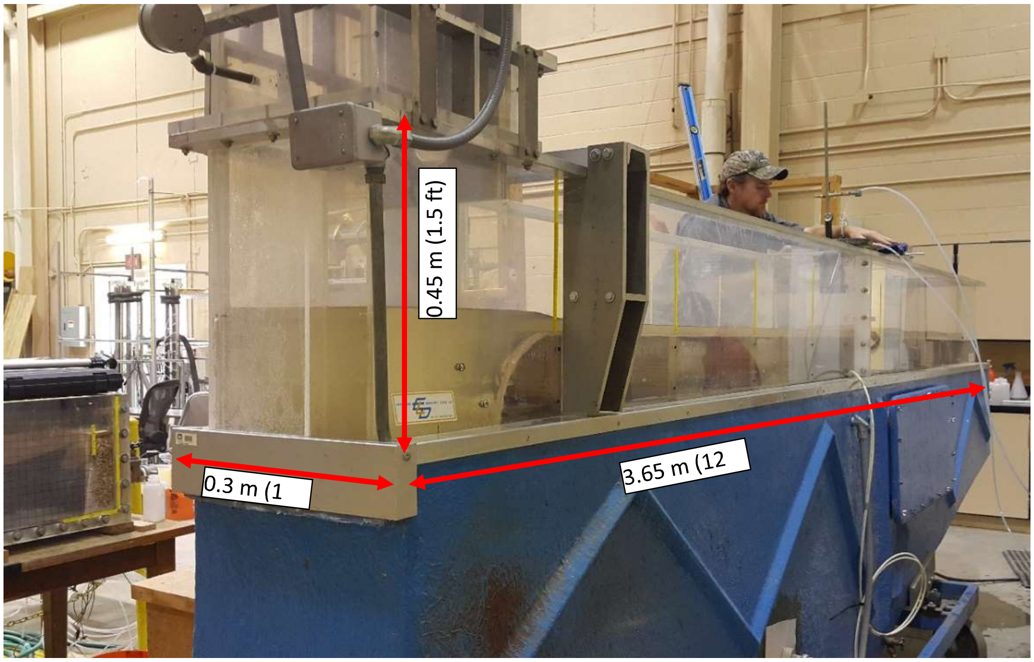

Figure 3. Small Flume showing Dimensions

A solution for the energy equation in the form of a first-order ordinary differential equation was used to check these measurements assuming a Manning's *n* value of 0.024. Equation 2 calculates the bed shear τ using a discrete form of the momentum equation (Hughes, 2017). After the test was stopped, the soil surface in the box was mapped using point gage measurements on a one-inch scale along the location where the maximum erosion occurred. More details are presented in Ellithy et al. 2018.

$$\tau = \frac{\gamma}{2}(y_1 + y_2)cos\theta\ sin\theta + \frac{\gamma}{2}\frac{cos^4\theta}{\Delta x}(y_1^2 - y_2^2) + \frac{\gamma q^2}{g\ \Delta x}\left(\frac{1}{y_1} - \frac{1}{y_2}\right) \quad (2)$$

where, *y1*, *y2* = vertical flow depth at locations 1 and 2 [*L*], *Δx* = horizontal distance between locations 1 and 2 [*L*], *γ* = specific weight of water [*F*/*L*3], *θ* = angle of bed relative to horizontal [radians], *q* = discharge per unit width [*L*2/*T*], *g* =gravitational acceleration [*L*/*T*2

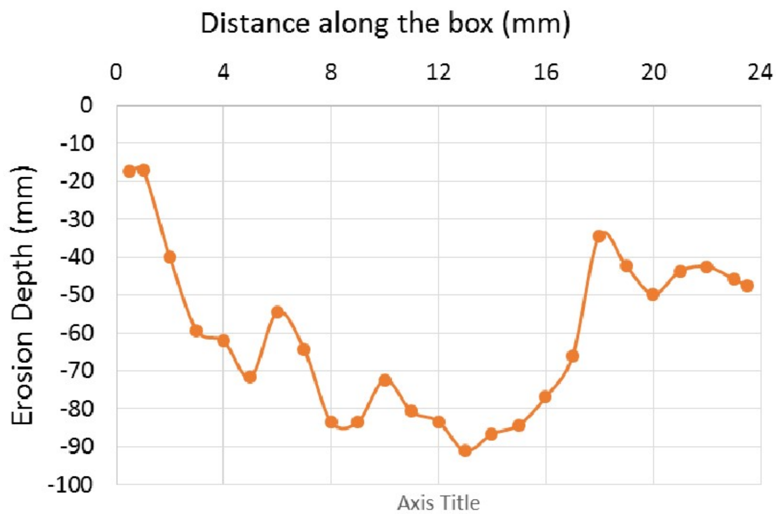

Figure 4. Erosion profile, mix 1-3, q= 0.0269 m^3/sec/m, slope 6%

RESULTS AND DISCUSSION

The velocity and water depth profile along the flume was matched with the solution of the energy equation for all the twelve conducted tests (three mixes and four hydraulic loadings each). Erosion rate was calculated by dividing the average erosion depth along the box by the time duration of the test. It should be noted that the measured erosion was observed to be uniform in some cases where the flow rate and acting bed shear was small, however, as the flow rate increased or the flume bed was tilted resulting in a higher velocity and higher bed shear, the profile of the erosion became more irregular along the soil surface resulting in a variation in the hydraulic loading which in turn resulted in a more irregular eroded surface as shown in Figure 4.

Figures 5.a and 5.b show the calculated average bed shear along the box for each of the twelve tests versus the average erosion rate. A linear equation was fit to the test results for each of the three mixes in Figure 5.a, and a bi-linear equation in Figure 5.b. The best fit of Equation (1) resulted in a critical shear stress τ_c of 1.5, 3.5 and 20 Pa for mixes 1-1, 1-2, and 1-3, respectively. And erodibility coefficient k_d of 2 cm^3/N-sec for mixes 1-1, and 1-2, and 1 cm^3/N-sec for mix 1-3. These values would classify the three mixes as “very erodible” according to Hanson and Simon,

2001. Attempting to fit a bi-linear equation to the test data where the smaller range of the acting bed shear stress was fit in one linear equation and the higher range in another resulted in a better fit as shown in Figure 5.b. This type of fitting needs a larger number of data points which make the erodibility parameters inconclusive at this point.

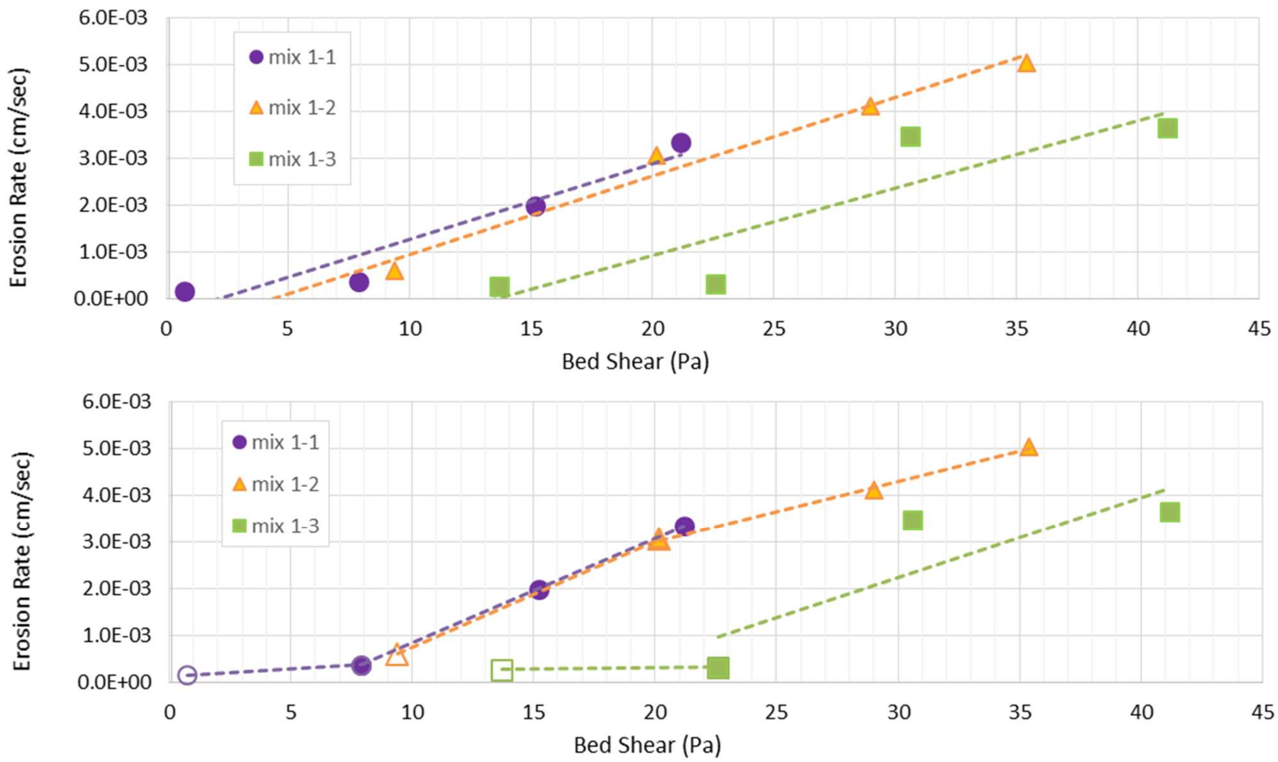

Figure 5. Erosion Rate a. linear equation, b. bi-linear equation

Figure 6 presents the test results on a semi log graph together with a nonlinear equation that calculates the dimensionless erosion rate $E*$ in terms of the dimensionless shear stress $\tau*$ as follows:

$$E^* = a\tau^{*b} \quad (3)$$

where $E^* = \frac{E_b}{D\sqrt{gRD}}$, E_b is the volumetric erosion rate in $cm^3/sec/cm$ (average erosion depth x eroded area/ width of the box), D is the mean soil diameter = 0.2 cm, g= gravitational acceleration= 981 cm/sec^2, R= submerged specific gravity of the soil= 1.035, 1.163, and 1.196 for soil mixes 1-1, 1-2 and 1-3, respectively, and
where, $\tau^* = \frac{\tau}{D\gamma'}$, τ is the bed shear stress in Pa, γ' is the submerged unit weight of soil = 10151, 11408, and 11722 N/m^3 for soil mixes 1-1, 1-2 and 1-3, respectively, and
a, and b are fitting parameters.

Using Equation 3 to fit the test data of the three mixes resulted in fitting parameters *a* and *b* equal to 0.07, 0.05, 0.03 and 2.5, 2.25, 2.0 for mixes 1-1, 1-2, and 1-3, respectively.

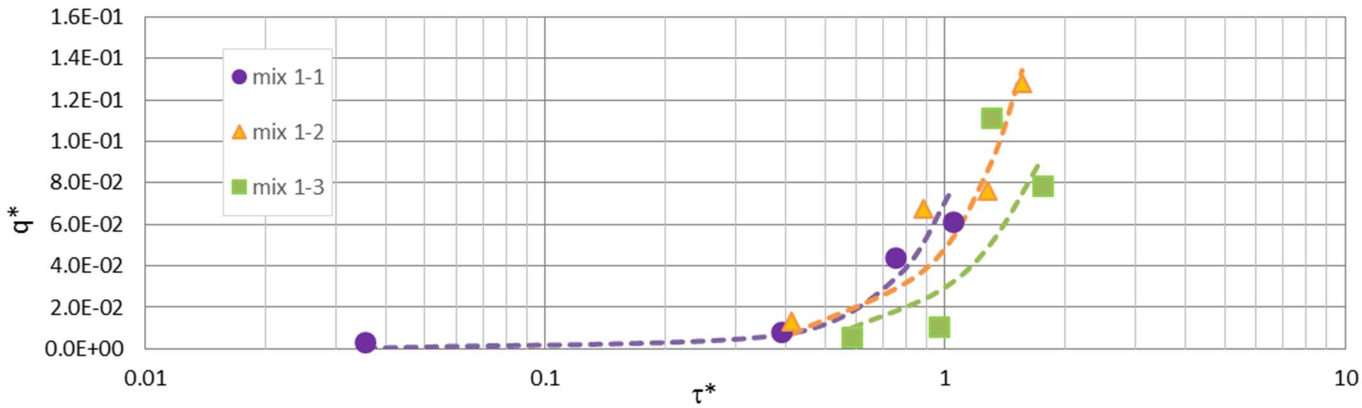

Figure 6. Non-linear erosion rate equation

Figure 5.a indicates that the presence of fines and clay in the sand mixes resulted in an increase in the critical shear τ_c and decrease in the erodibility coefficient k_d as the slope of the trend line passing all the data points for each mix. Although, the difference in k_d value between mixes 1-1 and 1-2 was not very obvious (both had a values of 2 cm^3/N-sec). However, it could be noticed that the rate of erosion is not uniform throughout the acting bed shear levels. As shown in Figure 5.b, a bilinear relationship between erosion rate and acting shear stress could be more representative of the erosion behavior of the tested sand mixes.

Examining the results from Figure 6, it could be noted that both fitting parameters *a* and *b* decrease as the fines and clay contents increase. This show that at a given shear stress, the mix with a higher fines content has lower erodibility and continues to erode in a slower rate. The dimensionless nature of this type of equation gives flexibility in using an exponent (parameter *b*) to relate the erosion rate to the acting bed shear stress without affecting the units balance as in linear Equation 1. Equation 3 does not contain the critical shear stress component of the erodibility, however this could have been embedded into both fitting parameters *a* and *b*. Similar testing on soil mixes with different mean soil diameter will allow this effect to be more clear. The nonlinear relationship seems to give a better and simpler model that represents the erosion rate throughout a wider range of acting shear stress and accommodates the effect of fines content.

SUMMARY AND CONCLUSIONS

In this paper, erosion rate results are presented from box testing on three soil mixes that have the same median grain size D_{50} of 2 mm, the fines content varies between zero to 20%, and the gravel content between zero to 30%. Each soil mix was compacted in the box near optimum water content and density as determined from standard Proctor. Each soil mix was tested several times at varying hydraulic loading ranging from 0.0028 to 0.028 m^3/sec (0.1-1 cfs) to determine the erosion rate after equal time intervals where the erosion rate was calculated by dividing the average erosion depth by the duration of the test. The acting bed shear stress was calculated using a discrete form of the momentum equation.

In general, the results indicate that the presence of fines and clay in the sand mixes resulted in an increase in critical shear stress and decrease in the erosion rate. Linear (excess shear), bi-linear and non-linear models were fit onto the test results. The dimensionless nature of the nonlinear model gives flexibility in using an exponent to more accurately relate the erosion rate to the acting bed shear stress. Critical shear stress of each mix could be embedded into both fitting parameters *a* and *b* of the nonlinear model (Equation 3). The nonlinear relationship seems to give a better and simpler model that represents the erosion rate of sand mixes throughout a wider range of acting shear stress and accommodates the effect of fines content. Future testing on sand and gravel mixes will to confirm the findings of this paper.

REFERENCES

ASTM. (2012). "Standard test method for Laboratory Characteristics of Soil Using Standard Effort (12,400 ft-lbf/ft^3 (600 kN-m/m^3)." American Society for Testing and Materials Standard Designation D 698-12, West Conshohocken, PA.

ASTM. (2007). "Standard test method for erodibility determination of soil in the field or in the laboratory by the Jet Index method." American Society for Testing and Materials Standard Designation D 5852-07, West Conshohocken, PA.

Ellithy, G.S., Wibowo, J.L. Corcoran, M.K. 2018. "Determination of Erosion Parameters of Coarse- Grained Materials Using a Small Flume", *Protections 2018 Conf Proceedings, UK*. 6-8June.

Ellithy, G.S., Savant, G., Wibowo, J.L. 2017. "Effect of Soil Mix on Overtopping Erosion", *ASCE EWRI*, Sacramento, CA 21-25 May.

Hanson, G.J., and Simon, A. (2001). "Erodibility of cohesive streambeds in the loess area of the Midwestern, USA". Hydrological Processes, p 23-38.

Hanson, G.J., Robinson, K.M., and Cook, K.R. (2001). "Prediction of headcut migration using a deterministic approach," *Transaction of the ASAE*, 44(3), 525-531.

Hughes, S.A. (2017). "Review of Proposed Physical Model to Evaluate Overtopping Erosion of Coarse-grained Materials". Report prepared for ERDC, water resources infrastructure technical program.

May, J.H. (1989). "Geotechnical Aspect of Rock Erosion in Emergency Spillway Channels." Report 4; Geologic and Hydrodynamics Controls on the Mechanics of Knickpoint Migration. Technical Report REMR-GT-3. Corps of Engineers, Waterways Experiment Station, Vicksburg, MS.

van Rijn, L.C. (1984). "Sediment pick-up functions." *Journal of Hydraulic Engineering* 110(10), 1494-1502.

van Rijn, L.C. (1993). "Principle of sediment transport in rivers, estuaries, coastal seas." Aqua Publications, Amsterdam, The Netherlands.

Visser, P.J., Ribberink, J.S., and Kalkwijk, J.P.Th. (1986). “Development of the breach and flow discharge in a dike-burst”. Rep. 8-86, Hydraulic and Geotechnical Eng. Div., Dept. Civ. Eng., Delft Univ. Tehn., Delft, The Netherlands.

Yalin, M.S. (1977). “Mechanics of sediment transport”. Pergamon Press, Oxford, England.